Ecological Informatics 86 (2025) 102979

Contents lists available at ScienceDirect

Ecological Informatics

journal homepage: www.elsevier.com/locate/ecolinf

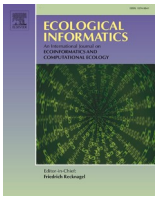

The dynamic driving mechanisms of wetland change from an asynchrony-spatiotemporal perspective: A case study in Pearl River Delta, China

Xiaoqing Yi [a,b,1], Yuhang Wang [c,**,1], Changjun Gao [a,b,*,2], Jiaojiao Ma [a,b], Demin Zhou [c], Christian J. Sanders [d], Guangjia Jiang [e], Zhongwen Hu [f], Junjie Wang [g], Haichao Zhou [g], Wei Li [h]

[a] Guangdong Provincial Key Laboratory of Silviculture, Protection and Utilization, Guangdong Academy of Forestry, Guangzhou 510520, China
[b] Guangdong Haifeng Wetland Ecosystem National Observation and Research Station, Guangzhou 510520, China
[c] College of Resource Environment and Tourism, Capital Normal University, Beijing 100048, China
[d] National Marine Science Centre, School of Environment, Science and Engineering, Southern Cross University, Coffs Harbour, NSW 2450, Australia
[e] South China Sea Environment Monitoring Center, State Oceanic Administration, Guangzhou 510300, China
[f] MNR Key Laboratory for Geo-Environmental Monitoring of Great Bay Area, Shenzhen University, Shenzhen 518060, China
[g] College of Life Science and Oceanography, Shenzhen University, Shenzhen 518060, China
[h] Institute of Wetland Research, Chinese Academy of Forestry, Beijing 100091, China

ARTICLE INFO

Keywords:
Wetland change
Driving mechanisms
Partial least squares structural equation modeling
Pearl River Delta
Remote sensing

ABSTRACT

The mechanism of wetland distribution (WD) has been well studied, but further research is needed on the mechanism of wetland change (WC). This study developed a model of the impact of changes in human activity (HA) and natural environment factors on WC from an asynchronous–spatiotemporal perspective, integrating remote sensing technologies and partial least squares–structural equation modeling (PLS–SEM). In the model, HA was reflected by economic and population data. The natural environment was reflected by the fundamental natural environment (FNE), which was mainly based on terrain, and the non-stable natural environment (NNE), which was mainly based on hydrological and temperature conditions. The model met the accuracy requirements in the Pearl River Delta (PRD). The results showed that there were differences in the response of WD and WC to driving factors from 1980 to 2020 in the PRD. FNE had a negative impact on WD, however, FNE changes (FNEC) had a positive impact on WC (mainly wetlands decrease). HA could affect NNE and subsequently WD, but NNE changes (NNEC) only began to affect WC after 2010. HA had a negative impact on WD and WC from 1980 to 2010, but both negative and positive impacts existed after 2010. By coupling areas of HA changes (HAC) with wetland decrease, it was found that HA should be restricted in the southeast of Foshan (areas where HA increase led to wetland decrease) to protect wetlands; The junction between Zhaoqing and Foshan (areas where HA decrease lead to wetland decrease) requires investment in improving the natural environment. The model proposed in this study can be applied to other areas with severe wetland degradation from HA and natural conditions, to assist in local wetland restoration and management.

* Corresponding author at: Guangdong Provincial Key Laboratory of Silviculture, Protection and Utilization, Guangdong Academy of Forestry, Guangzhou 510520, China.
** Corresponding author.
E-mail addresses: 2220902167@cnu.edu.cn (Y. Wang), gaochangjun@sinogaf.cn (C. Gao).
[1] These authors contribute equally to this work.
[2] Postal address: Guangdong Provincial Key Laboratory of Silviculture, Protection and Utilization, Guangdong Academy of Forestry, Guangzhou 510520, China; Guangdong Haifeng Wetland Ecosystem National Observation and Research Station, Guangzhou 510520, China.

https://doi.org/10.1016/j.ecoinf.2024.102979
Received 12 August 2024; Received in revised form 21 December 2024; Accepted 22 December 2024
Available online 28 December 2024

1. Introduction

Wetlands are critical for regulating resources, purifying water, storing carbon (Tan et al., 2023), moderating climate (Li et al., 2023), and maintaining biological diversity (Zhang et al., 2023a). Thus, wetlands ecosystems are vital both for humans and nature. However, the distribution and function of wetlands are vulnerable to changes (Erwin, 2009). Approximately 50 % of the world's wetlands have been lost since 1900, and 35 % since 1970 (Winkler and Dewitt, 1985; Zedler and Kercher, 2005). The net percentage of wetland loss ranges between 28 % and 87 % since 1700 according to recent estimates (Fluet-Chouinard et al., 2023; Hu et al., 2017; Sterling et al., 2013). Although individual researchers differ as to exactly how much of the world's wetlands have changed, a significant change in the area of wetlands has undoubtably occurred over the past decades.

Changes in the natural environment and human activity (HA) are two general factors leading to wetlands change (WC) (Asselen et al., 2013; Thomas et al., 2017). Natural environments such as climate and terrain have a significant impact on wetlands by altering their hydrology, vegetation, and even soil conditions (Erwin, 2009; Xu et al., 2024; Zhang, 2015). HA, such as urbanization, farmland reclamation, and grazing, can encroach on wetlands, resulting in irreversible damage to wetland conditions (Aktas and Donmez, 2019; Zhang et al., 2023b). Most researchers focus on the relationship between wetland distribution (WD) and driving factors from a static perspective. Some have studied the driving mechanisms of WD at the national scale, while others have conducted detailed studies using internationally important wetlands areas as cases. A direct relationship exists between WC and driving factors: once the driving factors change, WC may follow immediately. However, further research is needed to quantify the impact of changes in driving factors on WC from an asynchronous–spatiotemporal perspective; for example, the relationship between increased HA and decreased wetlands in a specific location during a specific period, or the relationship between changes in environmental factors and increased wetlands. The degree, time, and location of WC influenced by HA or natural environment factors can be directly quantified on the basis of the asynchronous–spatiotemporal driving mechanism, which is critical for wetland management and restoration.

Satellite remote sensing technologies provide unique opportunities for wetland monitoring over large areas efficiently and cost-effectively (Chen et al., 2014; Deng et al., 2023; Ma et al., 2023). At present, a series of coastal wetland mapping products of single surface type have been produced globally, nationally, or regionally, including water (Pickens et al., 2020), mudflat (Murray et al., 2022), mangroves (Bunting et al., 2022; Jia et al., 2023) and salt marshes (Mcowen et al., 2017). In terms of mapping multiple types of wetlands in inland areas, (Zhang et al., 2024) used time-series Landsat satellite images to present for the first time a global 30 m annual wetland map (named GWL-FCS30D) with a long time series (2000−2022) and eight wetland subcategories. Land use, nighttime lighting, and residential density can be obtained from remote sensing technologies, and setting different weights on these data can generate kilometer-scale grid data for gross domestic product (GDP) and population(Wang et al., 2016). These types of grid data have a high spatial resolution and can display the distribution of micro-level driving factors within administrative regions (Liu et al., 2005). The spatial heterogeneity of the driving mechanisms of WC can be shown using these remote sensing grid data. However, there is currently no available mapping of the Pearl River Delta (PRD) wetlands from 1980.

We used remote sensing technology to map the distribution of wetlands. There are both qualitative and quantitative methods to explore the impact of the natural environment and HA on WC. The driving force pressure state impact response (DPSIR) method is mainly used in qualitative research. The basic idea of the DPSIR method is that social, demographic, and economic development can generate pressure (Lu et al., 2019). Pressure may have adverse effects, such as the release of chemicals, physical and biological agents, climate change, and land use change (Omann et al., 2009). Statistical methods such as partial least squares regression, partial correlation analysis, linear correlation, logistic regression, grey correlation, redundancy analysis, geographic detector model, and structural equation modeling (SEM) (Asselen et al., 2013; Cui et al., 2014; Li et al., 2020; Zhang et al., 2021) are used to quantitatively analyze the relationship between WC and explanatory variables. SEM is a quantitative statistical method for studying causal relationships among multiple factors. SEM can establish direct and indirect interactions between various factors compared with other methods (Hayes et al., 2017). In SEM, variables that can be directly observed are called explicit or observed variables, whereas variables that cannot be directly observed are called implicit or latent variables. Latent variables can be measured indirectly by using observed variables. Partial least squares–structural equation modeling (PLS–SEM) is a type of SEM that is suitable for non-normal data. Many studies have used PLS–SEM to investigate the causal relationship between the driving factors (e.g. natural environment, HA) and wetland distribution (Li et al., 2021; Wang et al., 2022a; Wang et al., 2022b; Zhang et al., 2023b). However, to our knowledge, the relationship between changes in driving factors and WC has not yet been explored using SEM.

Located on the southern coast of China, the PRD is an important coastal urban agglomeration with a dense river network and rich wetland resources. However, it has experienced rapid urbanization in the past 40 years. The wetland ecosystem in the PRD is facing increasingly severe human stress. The process and driving factors of change need to be explored to better protect and manage wetlands. Therefore, this study took the PRD as the study area, analyzed the wetland change process in the PRD from 1980 to 2020, and explored the causal relationship between WD, WC, and driving factors based on PLS–SEM. This study aimed to: 1) analyze the spatiotemporal distribution of wetlands in the PRD from 1980 to 2020; 2) explore the impact of HA and the natural environment on WD and WC in the PRD over the past 40 years; 3) identify the coupling relationship between HA changes (HAC) and WC from a spatiotemporal perspective, and provide suggestions for wetland restoration and management.

2. Material and methods

2.1. Study area

The PRD (112°22′–115°25′ E, 21°28′–24°26′ N) is located in the southeast of Guangdong province, in the lower reaches of the Pearl River, adjacent to Hong Kong and Macao. It consists of nine cities in

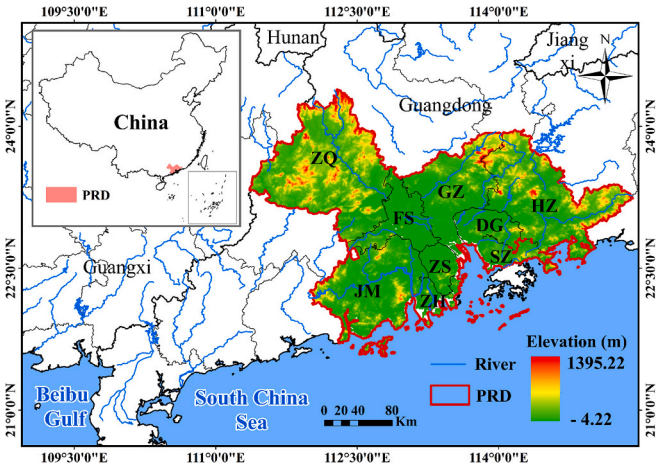

Fig. 1. Location of the Study area.
Note: Dongguan (DG), Foshan (FS), Guangzhou (GZ), Huizhou (HZ), Jiangmen (JM), Shenzhen (SZ), Zhaoqing (ZQ), Zhongshan (ZS), and Zhuhai (ZH).

Guangdong (Fig. 1). The PRD is formed by a central plain surrounded by hills, mountains, and islands. It belongs to a subtropical climate with high temperatures and abundant rainfall. The average annual temperature is 21–23 °C, and the average annual precipitation is over 1500 mm. In terms of topography and hydrology, it is characterized by a good water network with multiple channels, and there are a variety of wetland types, including coastal wetlands, river wetlands, paddy field wetlands, lake wetlands, and swamp wetlands. This study only considered wetland types within the land boundary of the PRD owing to the unique hydrological and distribution characteristics of coastal wetlands.

The PRD carries 74 % of the population in Guangdong province and contributes 88 % of Guangdong's economy. In addition, the PRD is characterized by high temperature and humidity, frequent rainfall, and frequent extreme weather events. Therefore, it is a typical case for studying the spatiotemporal distribution and causes of wetland changes under the influence of HA and climate change, which has important scientific significance for global wetland protection and management.

2.2. Methods

In this study, we identified the spatiotemporal changes of wetlands in the PRD from 1980 to 2020 and explored how natural factors and HA affected the WD and WC. We adopted an asynchronous spatiotemporal perspective to explore the influencing factors of wetland change. First, seven wetland categories were defined, and the wetland distribution was mapped using the random forest algorithm based on Landsat images. Second, various indicators of natural and HA factors affecting wetland distribution were established on a 5 km × 5 km grid scale using spatial statistical analysis methods. Third, correlation analysis and PLS–SEM were used to explore the driving mechanisms of wetland distribution and change, and the reliability of the results was evaluated. Finally, the spatial distribution of HAC areas and wetland degradation areas was coupled, and targeted suggestions are proposed for wetland restoration and management in the PRD. The technical roadmap of this study is shown in Supplementary Fig. S1.

2.2.1. Wetland distribution dataset

Remote sensing techniques were used to map the distribution of wetlands. First, Landsat surface reflectance images from 1980, 1990, 2000, 2010, and 2020 were chosen from the U.S. Geological Survey (http://earthexplorer.usgs.gov/) and geospatial data cloud websites (http://www.gscloud.cn/search). The images were selected with cloud cover less than 10 % and pre-processed through geometric and atmospheric correction. Second, a wetland classification system suitable for land cover characteristics within the land boundary was established, dividing wetlands in the PRD into seven categories: reservoir and ponds, forested wetland, paddy fields, river, lake, shrub swamps, and marsh (Supplementary Table S1). The random forest algorithm was used for the classification process in R Studio (https://valentinitnelav.github.io/satellite-image-classification-r/). Third, accuracy was assessed on the basis of field investigations and the visual interpretation of high-resolution historical images (Google Earth) and topographic maps.

2.2.2. Driving factors dataset

This study mainly explored two driving mechanisms related to WD and WC. The spatiotemporal distribution of the natural environment and HA was used to explore the impact on the WD, and the changes in these factors were used to explore the impact on WC. The driving factor data used are shown in Table 1. The natural environment included precipitation (Pre), temperature (Tem), elevation (DEM), Slope, and distance to rivers (Riv_dis). Slope was calculated from the elevation, and rivers were extracted from the Land use dataset. HA included distance to roads (national, provincial, county, rural, and other roads), distance to urban centers, population density (Pop), and GDP. In the process of establishing the road network database in 1990 and 2009, the road traffic map of the PRD and the traffic travel map of Guangdong province were geo-referenced, ortho-rectified, and digitized. The road network data for the remaining years were based on these two years and obtained through visual interpretation and vectorization using Landsat series images and Google Earth images. City point data was taken from Baidu maps. We also collected GDP and Pop data at the urban, county, and street levels from 1980 to 1990 from the government statistical yearbooks in addition to kilometer grid GDP and Pop products. Statistical yearbook data were used to perform linear interpolation on 1980 (the year with missing GDP and Pop grid data), and the interpolated data were used to analyze the mechanism of driving factor changes and WC.

Table 1
Data used in the study and their sources.

Driving factor	Data name	Data source	Data description
Pre	Precipitation	National Tibetan Plateau Data Center (https://data.tpdc.ac.cn/zh-hans/data/faae7605-a0f2-4d18-b28f-5cee413766a2)	1980-2020 1 km spatial resolution
Tem	Temperature	National Tibetan Plateau Data Center (https://data.tpdc.ac.cn/zh-hans/data/71ab4677-b66c-4fd1-a004-b2a541c4d5bf)	1980-2020 1 km spatial resolution
DEM, Slope	Elevation	Data Center for Resources and Environmental Sciences of Chinese Academy of Sciences (https://www.resdc.cn/data.aspx?DATAID=284)	SRTM 90 m spatial resolution
River	Land use	Data Center for Resources and Environmental Sciences of Chinese Academy of Sciences (https://www.resdc.cn/DOI/DOI.aspx?DOIID=54)	1980-2020 30 m spatial resolution
Road	Road network	Road traffic map of PRD Transportation and travel map of Guangdong province	Five levels of hierarchy
City center	City center point	Baidu map	2020
GDP, Pop	Socioeconomic factors (grid data)	Resource and environment science data platform (https://www.resdc.cn/DOI/DOI.aspx?DOIID=33, https://www.resdc.cn/DOI/DOI.aspx?DOIID=32)	1990-2020 1 km spatial resolution
GDP, Pop	Socioeconomic factors (statistical yearbook data)	Official websites of Guangdong provincial and local municipal governments	1980–2020 Province, city, county

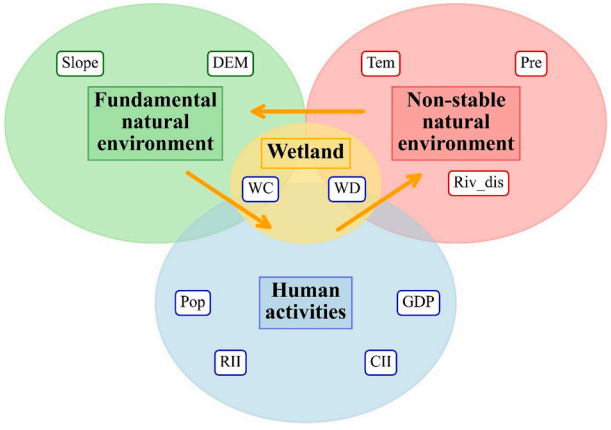

Fig. 2. Conceptual diagram of PLE-SEM of wetland distribution and changes driving mechanism.

2.2.2.1. Calculation of RII. The impact of HA on the natural environment is usually stronger in areas closer to roads. Different levels of roads have different impacts on the environment because they have different functions. For example, the impact of a highway on a certain location is generally greater than that of a rural road at the same distance. In this study, roads were divided into six levels: highways, national roads, provincial roads, county roads, rural roads and below, and other roads. We calculated the shortest distance between each grid in a resolution of 5 km × 5 km and different types of roads. If the distance was greater than 15 km, the shortest distance between the pixel and the road was specified as 15 km because when the shortest distance between a certain location and a road exceeded 15 km, the impact of the road on this location could be ignored(Yang et al., 2021). The total impact of each type of road was calculated on the basis of the road impact index (RII) proposed by Yang et al. (Eq. (1)).

$$RII = \sum_{i=1}^{6} w_i * \left(1 - \frac{D_{Ri}}{15}\right) \tag{1}$$

where RII represents the total impact of each type of road on pixels; a larger RII equates to a stronger the impact of the road on that pixel. i represents the type of road. w_i represents the weight of different types of roads on pixel points given by(Li et al., 2018) with the highways at 0.23, the national roads at 0.21, the provincial roads at 0.18, the county roads at 0.12, the rural roads and below rural roads of 0.09, and other roads at 0.04. D_{Ri} represents the closest distance between a pixel point and the road. The RII of 1980 was only calculated on the basis of national highways because only national highway data were collected in 1980.

2.2.2.2. Calculation of CII. Mao et al. (2021) studied the radiation range of central cities in 2021. The first-tier cities in the radiation range were Shenzhen and Guangzhou, with distances of 61.23 km and 51.08 km, respectively; Second tier cities were Foshan (43.37 km), Zhaoqing (45.52 km), Huizhou (49.93 km), and Dongguan (41.16 km), with a radiation radius between 35 and 50 km; Third tier cities were those with a radiation radius of less than 35 km, namely Zhuhai (29.10 km), Jiangmen (28.09 km), and Zhongshan (26.04 km). The city impact index (CII), based on the radiation range of different cities, was calculated using Eq. (2).

$$CII = 1 - \frac{D_C}{D_A} \tag{2}$$

where CII represents the distance between the grid and the city center; a larger CII indicates a greater the impact of the city on the grid. D_C represents the distance to the city center, and D_A represents the radiation range of the city.

2.2.3. Degree of wetlands area change

The study area was divided into a 5 km × 5 km grid, and then a wetland area change degree index (WACDI) was developed to determine the degree of wetland area change in different regions. The WACDI referenced the mangrove restoration effectiveness index (MREI) by (Wang et al., 2023). The wetland change area over time within the grid was statistically analyzed, and the change was divided into two categories: wetland increase and decrease. According to Eq. (3), wetland changes were processed to obtain a value between −1 and 1. A value of 0 indicated non-wetland or no change in wetland area, a positive value indicated an increase in wetland area, and a negative value indicated a decrease in wetland area. A larger absolute value of WACDI indicated a greater degree of wetland area change (Wang et al., 2023).

$$\begin{aligned} WACDI &= \begin{cases} rescale(\Delta U, \{0,1\}), if \Delta U > 0 \\ 0, if \Delta U = 0 \\ rescale(\Delta U, \{-1,0\}), if \Delta U < 0 \end{cases}, rescale(x, \{a,b\}) \\ &= a + \frac{b-a}{x_{max} - x_{min}}(x - x_{min}) \end{aligned} \tag{3}$$

where WACDI represents the wetland area change degree index, and ΔU represents the area of wetland change in two years within the grid. x_{max} represents the maximum change in the area of all grid wetlands in all periods, and x_{min} represents the minimum change in the area of all grid wetlands, $rescale(x, \{a,b\})$ operator rescaled the variable x to the range of $\{a,b\}$.

2.2.4. PLS–SEM for wetland distribution and change

2.2.4.1. Conceptual model creation. The correlation between various driving factors and wetlands (WD, WC) was analyzed on the basis of Pearson correlation analysis. Then, a PLS–SEM model was used to quantify the causal relationship between driving factors (natural, anthropogenic) and wetlands, to reveal the driving mechanisms of WD and WC from 1980 to 2020. PLS–SEM usually includes measurement models and structural models. A measurement model is an explanatory model composed of implicit variables and explicit variables. The structural model is a path diagram reflecting the relationship between the effects of implicit variables.

The most basic assumption of this study was that both the natural environment and HA had a direct impact on WD and WC. Moreover, the interactions between the natural environment and HA factors, as well as within these factors, were considered, which had indirect impacts on WD and WC. Natural environment factors were divided into two parts: fundamental natural environment (FNE) and non-stable natural environment (NNE). FNE referred to terrain conditions, including DEM and slope. NNE included temperature and hydrological parameters (precipitation, temperature, distance to rivers). HA was divided into distance variables (distance to city center, distance to roads) and socioeconomic variables (GDP, Pop). The distances to city centers and roads were represented by CII and RII, respectively. For example, the FNE (terrain conditions) could directly affect WD. In addition, the terrain could limit HA, thus indirectly affecting WC. HA could directly affect wetlands and indirectly affect wetlands by affecting NNE (including hydrological and temperature conditions). These basic assumptions constituted the conceptual driving mechanism model of WD

Table 2
Area and change rate of various types of wetlands from 1980 to 2020.

Wetland type	Area (km^2)					Area change rate (%)				
	1980	1990	2000	2010	2020	1980–1990	1990–2000	2000–2010	2010–2020	1980–2020
Reservoir and ponds	4539.02	3738.37	4003.01	3811.19	4032.06	-17 %	7 %	-5 %	−6 %	−11 %
Forested wetlands	2.98	1.77	0	1.49	0.99	-40 %	−100 %	NaN	−33 %	−67 %
Paddy field	12,226.71	11,954.49	4917.51	4155.42	3757.44	-2 %	−59 %	−15 %	−10 %	−69 %
River	1733.25	1399.68	1222.84	1232.50	1407.14	-19 %	−13 %	0.7 %	14 %	−19 %
Lake	13.63	12.99	13.08	14.59	16.52	-5 %	0.7 %	12 %	13 %	21 %
Shrub swamps	0.75	0.66	0.67	0	0	-11 %	1 %	−100 %	NaN	−100 %
Marsh	30.68	28.79	28.73	18.05	17.77	-6 %	−0.2 %	−42 %	−2 %	−42 %
Total area	18,547.03	17,136.76	10,185.83	9233.23	9231.93	-8 %	−41 %	−9 %	0	−50 %

Note: 'NaN' means that the starting year area for calculating the growth rate is 0.

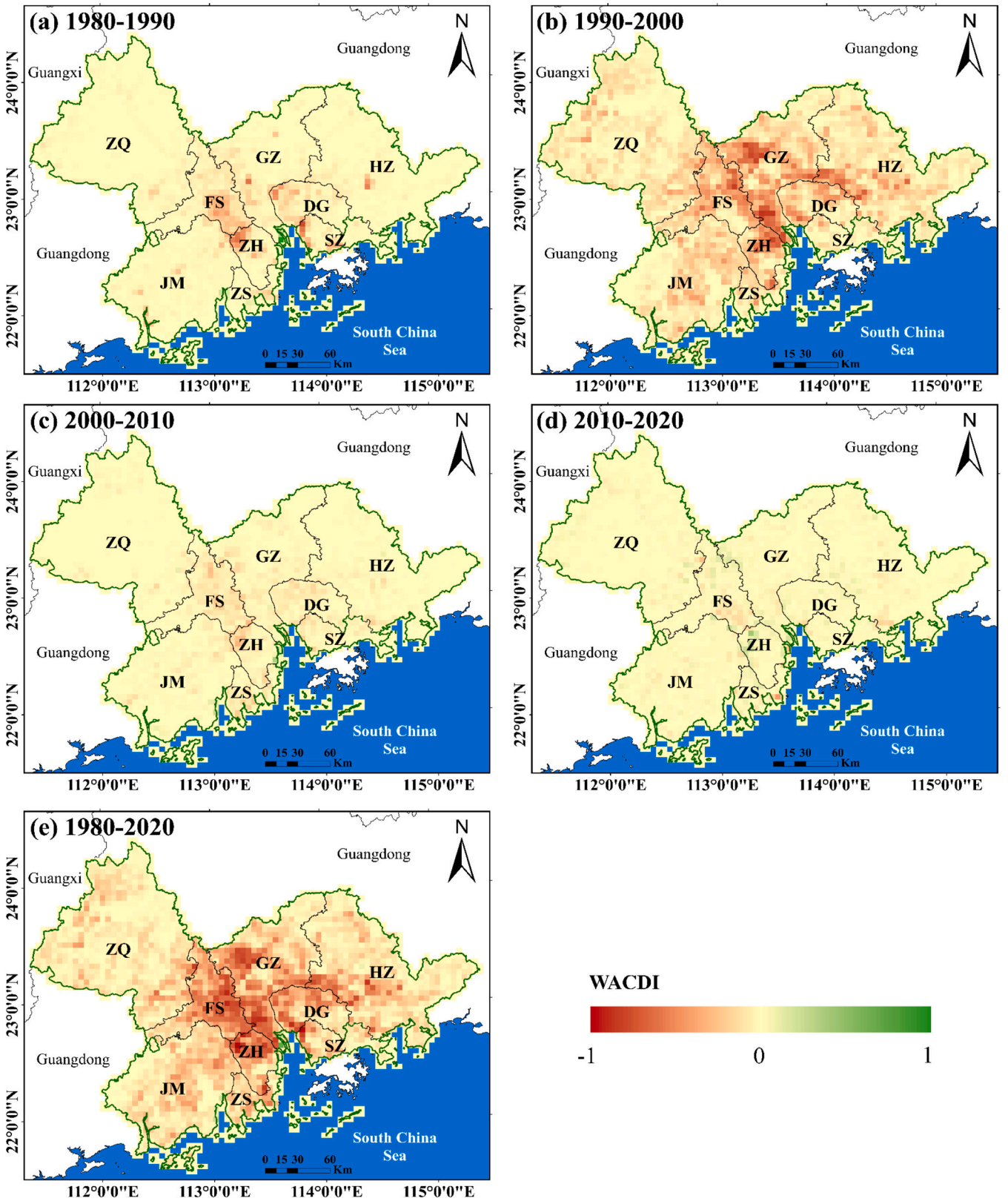

Fig. 3. Distribution map of WACDI during 1980–2020.

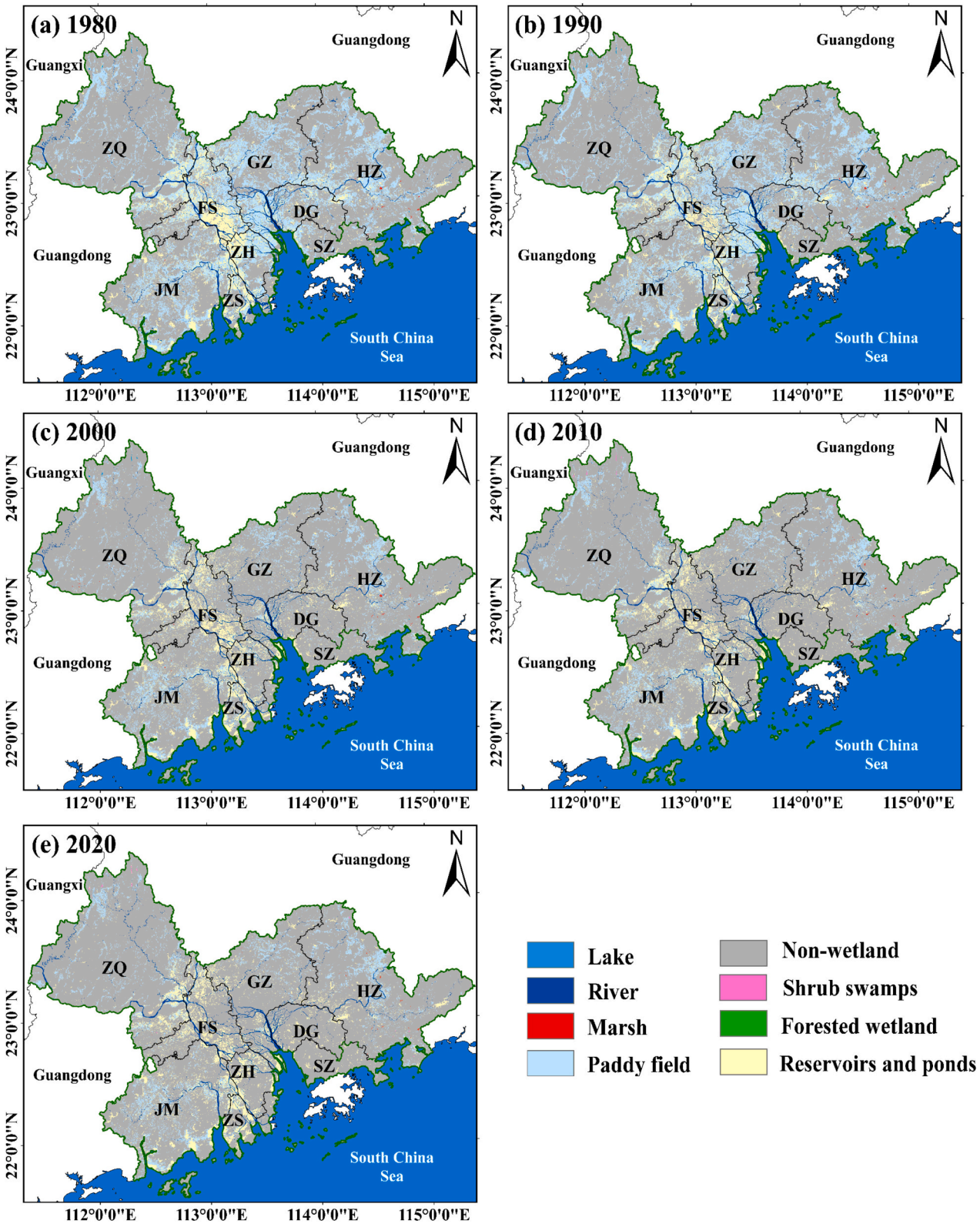

Fig. 4. Distribution map of wetland types during 1980–2020.

and WC through the interaction of natural environment and HA factors (Fig. 2). The values of driving factors and wetland area within each grid were used as input data for PLS–SEM to study the driving mechanism of WD. The specific numerical values of Tem, Pre, WC; and the degree of Riv_dis, RII, Pop, and GDP changes were used as input data to study the dynamic driving mechanism of WC.

2.2.4.2. Model validation and revision. The consistency and reliability of the model were evaluated using composite reliability (CR). The CR value is positively correlated with reliability, and a value of between 0.6 and 0.7 is commonly considered acceptable in exploratory research(Hair et al., 2011). Average variance extracted (AVE) was used to assess the conversion validity of each construction measure. An acceptable AVE

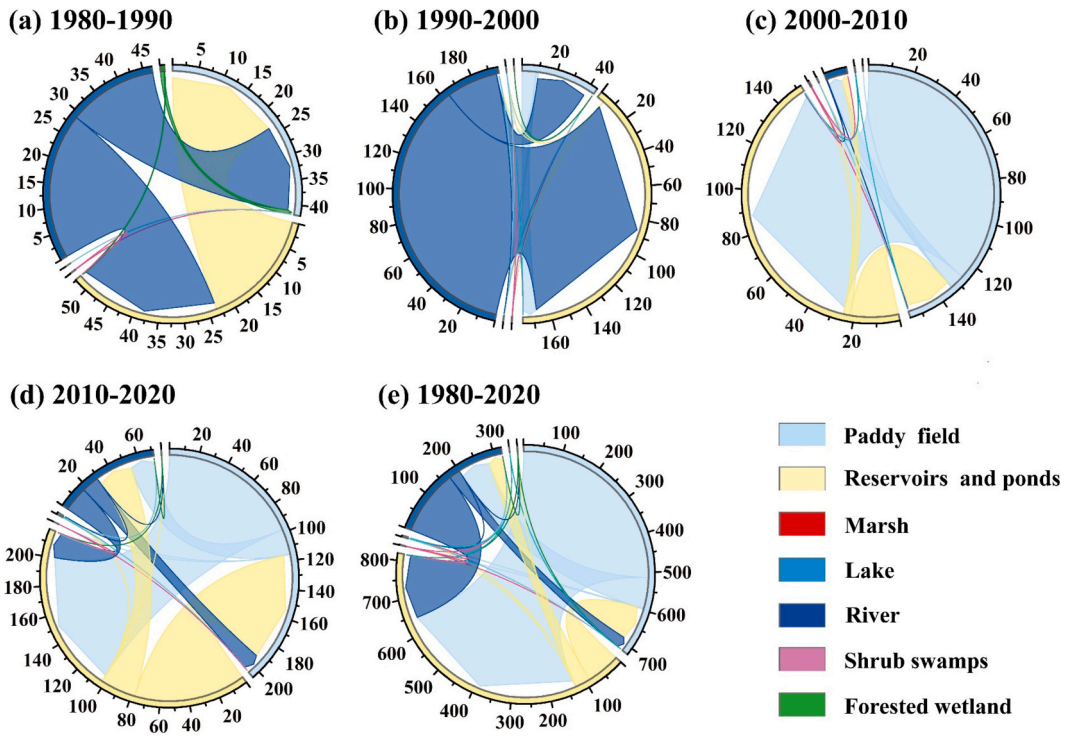

Fig. 5. The chord diagram of wetland-type transformation from 1980 to 2020. Note: (unit of area: km^2).

value is greater than 0.5, which indicates that the structure can explain at least 50 % of the differences in the model. In addition to AVE and CR, the variance inflation factor (VIF) was used to detect multicollinearity. A $VIF > 5$ means there is relatively high collinearity. A $VIF > 10$ indicates that the variable has severe collinearity and cannot be analyzed further (Hair et al., 2011).

3. Results

3.1. Spatiotemporal changes in wetlands in the PRD

3.1.1. Wetlands area change over time

The results showed that the producer accuracy ranged from 73.7 % to 90.0 %, and the user accuracy ranged from 77.8 % to 88.7 %. The overall accuracy was 85.9 %, and the Kappa coefficient was 0.82. The accuracy assessments demonstrated that the wetland classification maps mainly agreed with ground truth. Table 2 shows the area and change rate of various types of wetlands from 1980 to 2020. The total wetland area in the PRD for 1980, 1990, 2000, 2010, and 2020 was 18,547.03 km^2, 17,136.76 km^2, 10,185.83 km^2, 9233.23 km^2, and 9231.93 km^2, respectively. The decrease in total wetland area was the highest from 2000 to 2010, at 50 %; followed by 1990 to 2000, accounting for 41 %. The total wetland area change rate from 2010 to 2020 was less than 0.01 %. Reservoir and ponds, river, and shrub swamps all experienced at least one increase in area from 1980 to 2020 and lake area showed a 21 % increase overall from 1980 to 2020. Forested wetlands, paddy fields, and marsh all experienced a decrease in area from 1980 to 2020, and the area of shrub swamps decreased the most from 1980 to 2020.

3.1.2. Degree of wetlands area spatiotemporal change

Fig. 3 shows the degree of WC in the PRD from 1980 to 2020. Supplementary Fig. S2 shows the WC area in various cities of the PRD during 1980–2020. The overall wetland area mainly decreased from 1980 to 2020, with Guangzhou and Huizhou experiencing the largest loss in the area (Supplementary Fig. S2a). The increase in wetlands was the most significant during 2010–2020, with Jiangmen and Zhaoqing experiencing the largest increase in area (Supplementary Fig. S2b). The analysis of periods showed that the wetland area at the junction of Zhuhai and Foshan decreased significantly from 1980 to 1990, with a WACDI between −0.6 and − 0.4. The most significant loss in wetland area was during 1990–2000, concentrated in the western part of Guangzhou, the eastern part of Foshan, the northern part of Zhuhai, and the border area between Dongguan and Huizhou. The WACDI of these regions ranged from −0.8 to −0.6. From 2000 to 2010, although the change in wetland area was still mainly a decrease, the degree of decrease was significantly lower. The slowdown in wetland reduction was related to the slower pace of urban construction and the introduction of some wetland protection and restoration policies. The most significant increase in wetland area was during 2010–2020, concentrated in the northwest of Zhuhai and the western part of Guangzhou. The WACDI was between 0.1 and 0.4, and the cities with the highest increase in the area were Jiangmen and Zhaoqing.

3.1.3. Transformation between different wetland types

Fig. 4 shows the distribution and changes in various types of wetlands from 1980 to 2020. From 1980 to 2020, paddy fields and reservoirs and ponds had an extensive distributional range. Reservoirs and ponds were mainly distributed in the central western of the PRD, whereas paddy fields were mainly distributed in the central eastern area. Marsh was mainly scattered in the eastern area, and rivers had varying degrees of distribution in various areas. From 1980 to 1990, there was a significant decrease in reservoirs and ponds in the central western area. From 1990 to 2000, paddy fields experienced the most significant decrease, with the main loss occurring in the central area of the PRD. The overall changes in wetlands were relatively small during 2000–2010 and 2010–2020, compared with 1980–2000.

Fig. 5 shows the transformation between different types of wetlands from 1980 to 2020. The wetland types with the most significant transformation during 1980–2020 were river, paddy fields, and reservoirs and ponds. The main transformation occurred from river to paddy fields

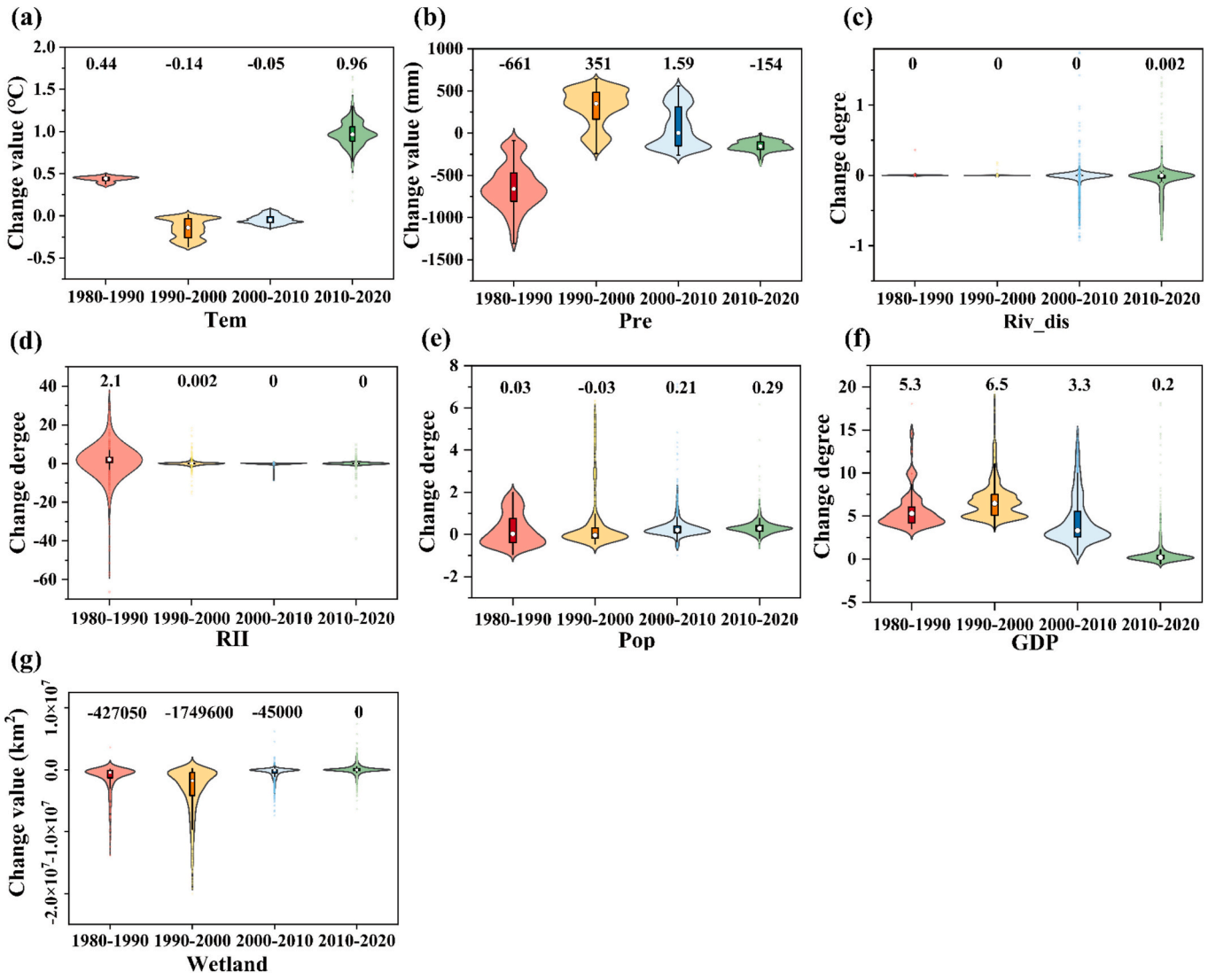

Fig. 6. The violin plot of changes in various driving factors and wetland area at different periods.

and reservoirs and ponds during 1980–1990 and 1990–2000, with conversion areas of 46.75 km^2 and 193.98 km^2. The conversion area from paddy fields to reservoirs and ponds was the highest during 2000–2010 and 2010–2020, with 126.82 km^2 and 97.97 km^2, respectively. From 1990 to 2020, the largest conversion area was from paddy fields to reservoirs and ponds, at 514.06 km^2, followed by the conversion area from river to reservoirs and ponds, at 171.45 km^2.

3.2. Relationship between driving factors and wetland distribution

3.2.1. Changes in driving factors

The violin plots as Fig. 6 show the differences in the driving factors change and WC at different periods. The variable change and WC in terms of minimum, maximum, median, and their distribution in four different periods (1980–1990, 1990–2000, 2000–2010, and 2010–2020), can be seen clearly. The median and overall distribution of change degree of GDP during the four different periods were all greater than 0, indicating an increasing trend of GDP in the entire region over time. The median change degrees of Pop, Riv_dis, and RII were around 0, and the shape of the violin was symmetrical, indicating that the changes in these driving factors both had increased and decreased. Overall, WC was less than 0 from 1980 to 2020, indicating that a decrease was the main trend during that time. The fluctuations in Pre and Tem changes were stronger than other factors, with more areas experiencing a decrease in Pre during 1980–1990, while there was mainly an increase from 1990 to 2020. The decrease in Tem during 1990–2000 was more pronounced, with an increase being the main trend during 1980–1990, 2000–2010, and 2010–2020.

3.2.2. Pearson correlation between the distribution of driving factors and wetlands

Fig. 7 shows the correlation between WD and various driving factors in the PRD from 1980 to 2020. Overall, factors that were highly correlated with WD from 1980 to 2020 included DEM, Slope, Tem, Riv_dis, and RII. There was a positive correlation between Tem, RII, and WD, while Slope, DEM, and Riv_dis were negatively correlated with WD. There was a negative correlation between Pre and WD in 1990, with a correlation coefficient of −0.39. There was a positive correlation between 1980, 2002, 2010, and 2020, with correlation coefficients of 0.19, 0.20, 0.042, and 0.11, respectively. Pop was positively correlated with WD in 1980, 1990, and 2000, with correlation coefficients of 0.37, 0.31, and 0.043, respectively. However, it was negatively correlated with WD in 2010 and 2020, with correlation coefficients of −0.030 and − 0.056. GDP showed a negative correlation with WD in 2020, with a correlation coefficient of −0.076. However, it showed a positive correlation in 1980, 1990, 2000, and 2010. The positive correlation coefficient

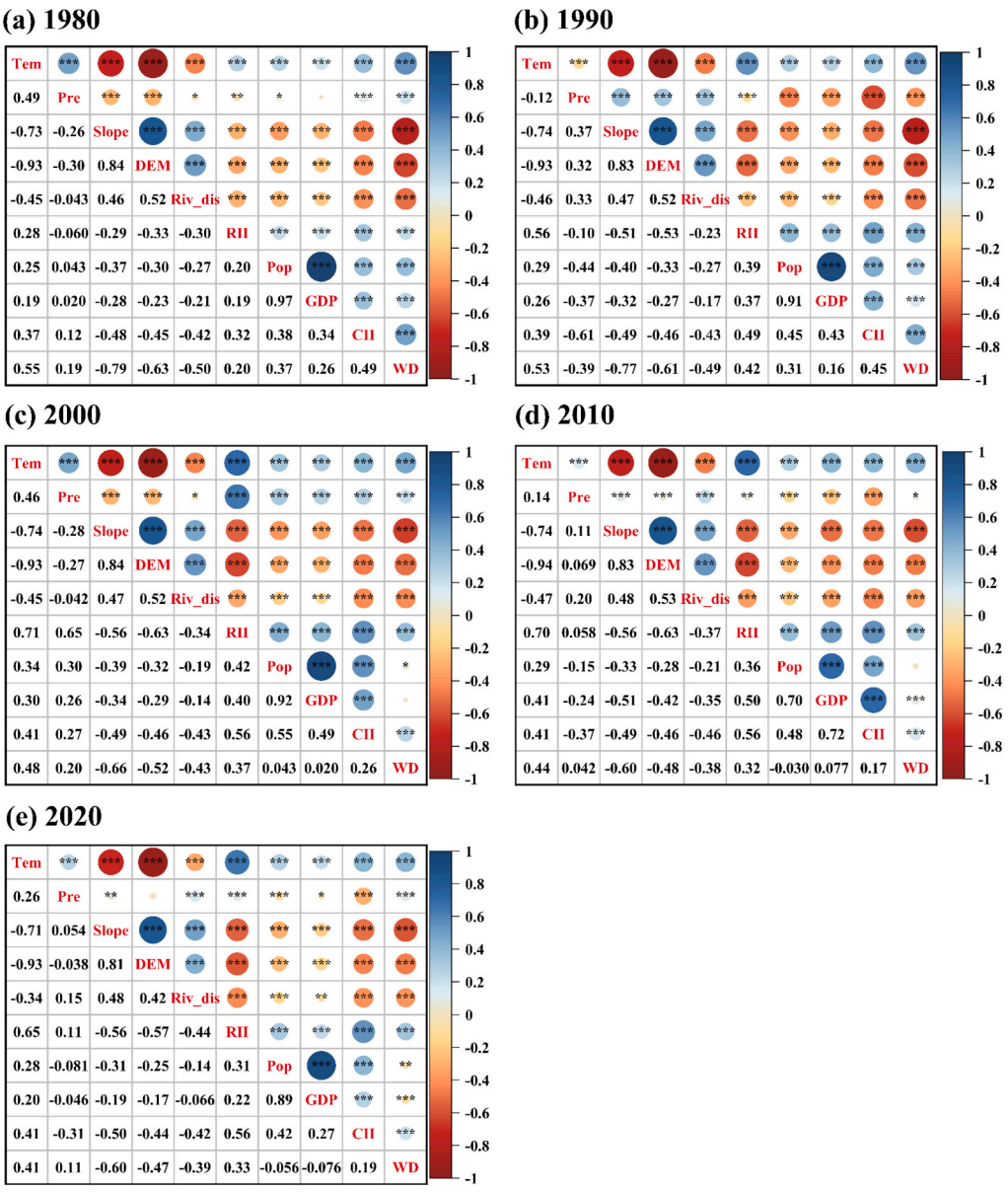

Fig. 7. Correlation between distribution of driving factors and wetlands.

decreased with time. There was a positive correlation between CII and WD from 1980 to 2020, but the positive correlation coefficient decreased over time. In addition, GDP, Pop, and CII were positively correlated with Tem, positively correlated with Pre in 1980 and 2000, and negatively correlated in 1990, 2010, and 2020.

3.2.3. Pearson correlation between the changes in driving factors and wetlands

Fig. 8 shows the correlation between changes in driving factors and WC in the PRD. From 1980 to 1990, PreC (Pre change), Slope, and PopC (Pop change) were positively correlated with WC, with correlation coefficients of 0.24, 0.33, and 0.17, respectively. CII and GDP were negatively correlated with WC from 1980 to 1990, with correlation coefficients of −0.45 and − 0.21. From 1990 to 2000, Slope, DEM, and Riv_disC (Riv_dis change) were positively correlated with WC, with correlation coefficients of 0.57, 0.46, and 0.017, respectively. The factors negatively correlated with WC during 1990–2020 included TemC, PreC, RIIC, PopC, GDPC, and CII, with correlation coefficients of −0.21, −0.37, −0.13, −0.074, −0.27, and − 0.50, respectively. From 2000 to 2010, the factors positively correlated with WC were TemC (Tem change), PreC, Slope, DEM, Riv_disC, and RIIC (RII change), with correlation coefficients of 0.25, 0.28, 0.44, 0.33, 0.18, and 0.019, respectively. The correlation coefficients between PopC, GDPC, and CII and WC were − 0.21, −0.27, and − 0.50, respectively. From 2010 to 2020, the factors positively correlated with WC were PreC, Slope, RIIC, and CII, with correlation coefficients of 0.021, 0.047, 0.0021, and 0.015, respectively. PopC and GDPC were not significantly associated with WC.

3.3. PLS–SEM for WD and WC in the PRD

3.3.1. PLS–SEM for the distribution of wetlands

The CR values of the potential variable NNE in 2010 and 2020 were 0.688 and 0.620, respectively. The CR values of each potential variable in the remaining years were greater than 0.7. All years had an AVE greater than 0.5. The VIF values were all below 10, indicating that there was no severe collinearity between the observed variables. Supplementary Tables S2 and S3 provide detailed information on the PLS–SEM accuracy and VIF of the driving factors and WD.

Fig. 9 shows the PLS–SEM of the direct impact of explicit and implicit variables on WD from 1980 to 2020. FNE had a direct negative impact

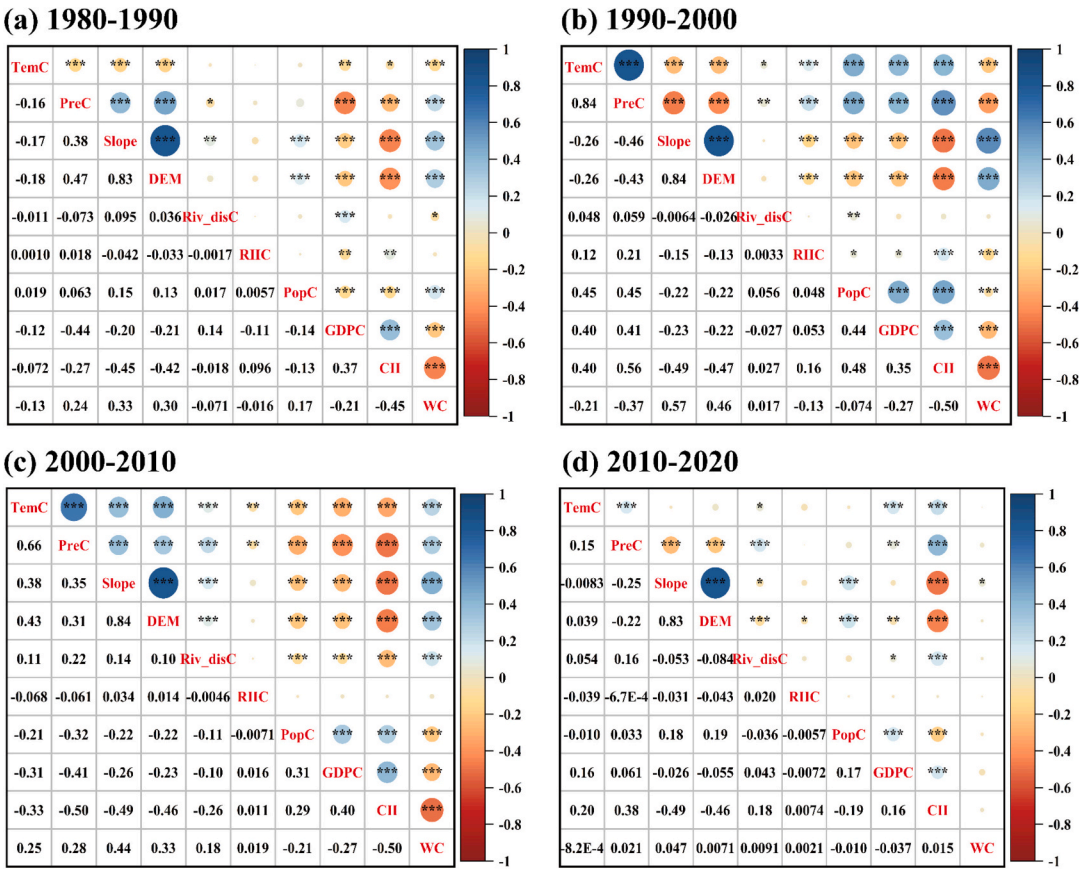

Fig. 8. Correlation between changes in driving factors and wetlands.

on HA from 1980 to 2020, with an impact coefficient of −0.615 to −0.864. NNE was directly positively affected by HA in 1980, 2000, and 2020, and was directly negatively affected in 1990 and 2010. Overall, the WD was influenced by three factors: FNE, HA, and NNE (except NNE in 2000). FNE and NNE had a negative impact on WD from 1980 to 2020, but the impact tended to weaken over time. HA had a positive impact on WD in 1980, but the impact was not significant in 1990 (p-value >0.01). It had a negative impact on WD from 1990 to 2020, and the degree of negative impact showed an upward trend over time.

Table 3 presents the direct, indirect and total effects among FNE, NNE, HA and WD based on the statistically significant SEM paths. The impact on NNE included both direct impacts from HA and indirect impacts generated by FNE through HA (FNE–HA–NNE) from 1980 to 2020. The impact coefficients in 1980, 1990, 2000, 2010, and 2020 were − 0.201, 0.307, −0.408, 0.282, and − 0.360, respectively. Both HA and FNE had an indirect impact on WD in 1980, 1990, 2010, and 2020. However, the only indirect pathway affecting WD in 2000 was FNE–HA–WD. Except for 2000, the only factor affecting WD was FNE, with the pathway being FNE–HA–WD, Both HA and FNE had an indirect impact on WD in 1980, 1990, 2010, and 2020. In terms of the total effect on WD from 1980 to 2020, the coefficient of influence of HA ranged from −0.286 to 0.114, and the negative impact gradually increased. The coefficient of influence of FNE ranged from −0.886 to −0.538, and NNE ranged from −0.231 to −0.123.

3.3.2. *PLS–SEM for the changes of wetlands*

Fig. 3 shows that some areas experienced an increase in wetlands from 2010 to 2020, with the degree of increase being more significant compared with other periods. The correlation between WC and the changes in various driving factors in Fig. 7 was mostly close to 0, without a single positive or negative correlation, reflecting the complex situation of WC. Moreover, the PLS–SEM results also indicated that only FNE had a significant impact on WC (p = 0.014) from 2010 to 2020, whereas the other latent variables (HA, NNE) were not significant. Therefore, we separately modeled and analyzed two WC scenarios: wetland increase and wetland decrease, to avoid the interference of internal consistency of the PLS–SEM caused by both increase and decrease in WC during 2010–2020. Fig. 10 shows the PLS–SEM of the impact of changes in driving factors on WC (Fig. 10d is wetland decrease during 2010–2020). The PLS–SEM model and accuracy assessment results of the impact of changes in driving factors on wetland increase during 2010–2020 are shown in Supplementary Tables S4, S5, and Fig. S3. The CR of each latent variable was greater than 0.7 and the AVE was greater than 0.5 during 1980–1990, 1990–2000, 2000–2010, and 2010–2020, except for the CR of NNEC and HAC during 2010–2020, which was 0.693 and 0.669. The VIF of all observed variables was less than 10 in all periods. The accuracy assessments and VIF of PLS–SEM for driving factor changes and WC are detailed in Supplementary Tables S6 and S7.

FNE had a direct negative impact on HAC from 1980 to 2020, with an impact coefficient of −0.421 to −0.505. HAC directly affected NNEC. There were negative impacts during 1980–1990 and 2000–2010, with impact coefficients of −0.412 and − 0.552, while there were positive impact coefficients of 0.597 and 0.401 during 1990–2000 and 2010–2020. FNE had a positive impact on wetland decrease from 1980 to 2020, with impact coefficients of 0.185 to 0.451. HAC had a direct negative impact on wetland decrease, with the strongest negative impact occurring during 2000–2010, with a coefficient of −0.370, and the weakest impact occurring during 2010–2020, with a coefficient of −0.172. NNEC did not have an impact on the decrease of wetlands from 1980 to 2010 but had a direct negative impact with a coefficient of −0.068 from 2010 to 2020. HAC had a direct positive impact on wetland increase during 2010–2020, with an impact coefficient of 0.201. FNE had a negative impact on wetland increase during 2010–2020, with a

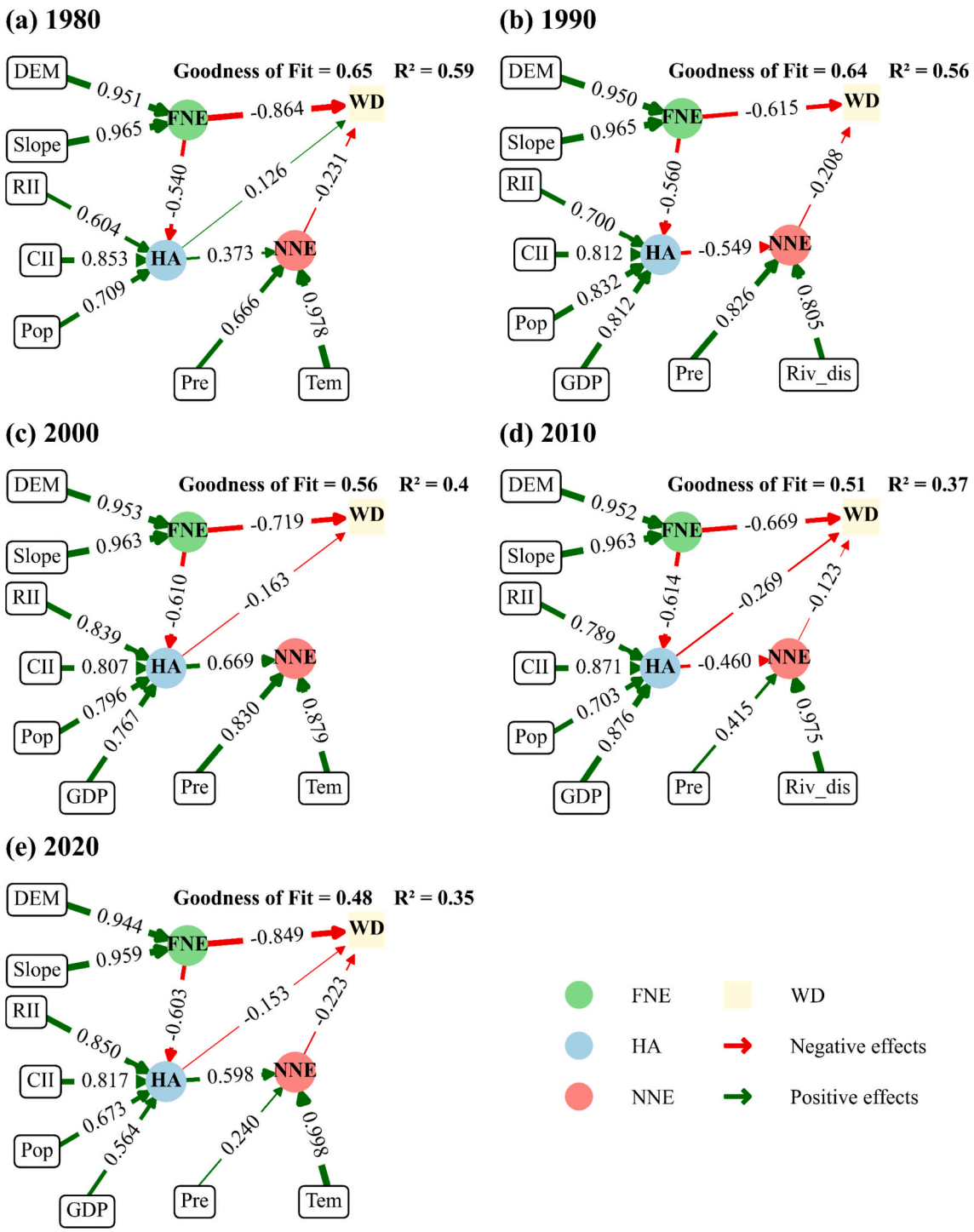

Fig. 9. PLS-SEM diagram of the relationship between each variable and the distribution of wetlands during 1980–2020. The significance level of all path coefficients is less than 0.001.

coefficient of −0.308 (Supplementary Fig. S3).

In terms of indirect impacts, FNE had a positive impact on WC by suppressing HAC (FNE–HAC–WC), with impact coefficients of 0.143, 0.092, 0.176, and 0.087 during 1980–1990, 1990–2000, 2000–2010, and 2010–2020, respectively (Table 4). FNE also had an impact on wetland decrease through HAC and NNEC during 2010–2020 (FNE–HAC–NNEC–WC), with an impact coefficient of 0.014. In addition, from 2010 to 2020, HAC had an impact of −0.027 on wetland decrease by affecting NNEC, and NNEC had an impact of −0.102 on wetland increase through HAC (Supplementary Table S8).

3.4. Coupling of human activities and wetland changes

We coupled HAC with wetland decrease areas from 2010 to 2020 based on the predicted results of PLS–SEM (Fig. 11-a). The areas where HA increased and wetland decreased simultaneously, accounted for 38.2 % of the total wetland area in the PRD during 2010–2020. These areas were densely distributed in the central part of the PRD and the southeastern part of Foshan. The increase in HA led to a significant loss in wetland area in the southern PRD and coastal areas of Zhuhai. In addition, 10.1 % of the regions experienced a simultaneous decrease in

Table 3
The direct, indirect and total effects among Fundamental Natural Environment (FNE), Non-stable Natural Environment (NNE), Human Activity (HA) and Wetland Distribution (WD) based on the statistically significant SEM paths.

Effect		Path	1980	1990	2000	2010	2020
Effect on HA	Direct	FNE-HA	−0.540	−0.560	−0.610	−0.614	−0.603
	Indirect	–	–	–	–	–	–
	Total	FNE ~ HA	−0.540	−0.560	−0.610	−0.614	−0.603
Effect on NNE	Direct	HA-NNE	0.373	−0.549	0.669	−0.460	0.598
	Indirect	FNE-HA-NNE	−0.201	0.307	−0.408	0.282	−0.360
	Total	HA ~ NNE	0.373	−0.549	0.669	−0.460	0.598
		FNE ~ NNE	−0.201	0.307	−0.408	0.282	−0.360
Effect on WD	Direct	HA-WD	0.126	–	−0.163	−0.269	−0.153
		NNE-WD	−0.231	−0.208	–	−0.123	−0.223
		FNE-WD	−0.864	−0.615	−0.719	−0.669	−0.849
	Indirect	HA-NNE-WD	−0.086	0.114	–	0.057	−0.133
		FNE-HA-WD	−0.068	–	0.099	0.165	0.092
		FNE-HA-NNE-WD	0.047	−0.064	–	−0.035	0.080
	Total	HA ~ WD	0.040^{ns}	0.114	−0.163	−0.212	−0.286
		FNE ~ WD	−0.886	−0.679	−0.620	−0.538	−0.677
		NNE ~ WD	−0.231	−0.208	–	−0.123	−0.223

NS, not significant.

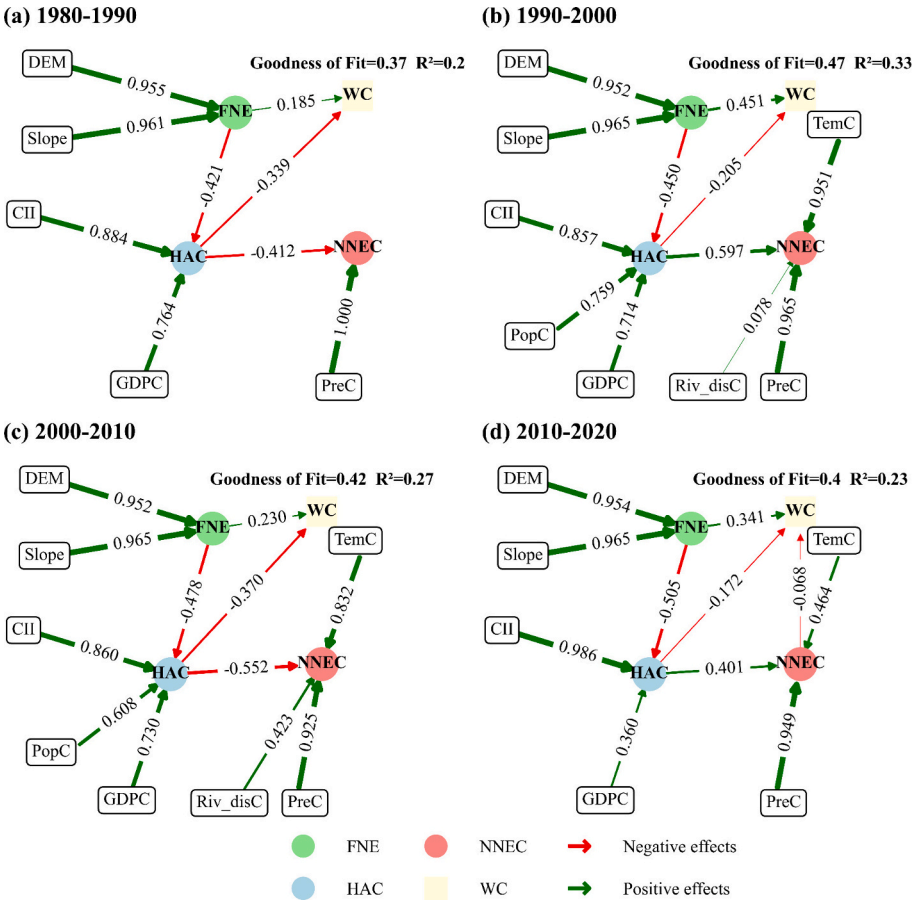

Fig. 10. PLS-SEM diagram of the relationship between each variable and the change of wetlands in an asynchrony-spatiotemporal period. The significance level of all path coefficients is less than 0.001.

HA and wetlands. This situation was more common at the junction of Zhaoqing and Foshan. The decrease of wetlands was mainly due to the transformation of reservoir and ponds into construction land (Supplementary Fig. S4). Similarly, we coupled the HAC with the wetland increases from 2010 to 2020. The results indicated that the areas where HA increased and wetlands increased accounted for 39.7 % of the total wetland area, which was slightly higher than 38.2 %. With the increasing awareness of wetland protection and restoration in the process of urban construction, wetland degradation was approximately balanced by wetland restoration. However, the average HA was smaller than in areas where wetlands decreased and HA increased simultaneously (Supplementary Fig. S5). The area with reduced HA and increased wetland area accounted for 12 %.

Table 4
The direct, indirect and total effects among Fundamental Natural Environment (FNE), Non-stable Natural Environment Change (NNEC), Human Activity Change (HAC) and wetland Change (WC) based on the statistically significant SEM paths.

Effect		Path	1980–1990	1990–2000	2000–2010	2010–2020
Effect on HAC	Direct	FNE-HAC	−0.421	−0.450	−0.478	−0.505
	Indirect	–	–	–	–	–
	Total	FNE ~ HAC	−0.421	−0.450	−0.478	−0.505
Effect on NNEC	Direct	HAC-NNEC	−0.412	0.597	−0.552	0.401
	Indirect	FNE-HAC-NNEC	0.173	−0.269	0.264	−0.203
	Total	HAC ~ NNEC	−0.412	0.597	−0.552	0.401
		FNE ~ NNEC	0.173	−0.269	0.264	−0.203
	Direct	HAC-WC	−0.339	−0.205	−0.370	−0.172
		`FNE-WC	0.185	0.451	0.230	0.341
		NNEC-WC	-	-	-	−0.068
Effect on WC	Indirect	FNE-HAC-WC	0.143	0.092	0.176	0.087
		HAC-NNEC-WC	-	-	-	−0.027
		FNE-HAC-NNEC-WC	-	-	-	0.014
	Total	HAC ~ WC	−0.339	−0.205	−0.370	−0.200
		FNE ~ WC	0.327	0.543	0.406	0.442
		NNEC~WC	-	-	-	−0.068

NS, not significant.

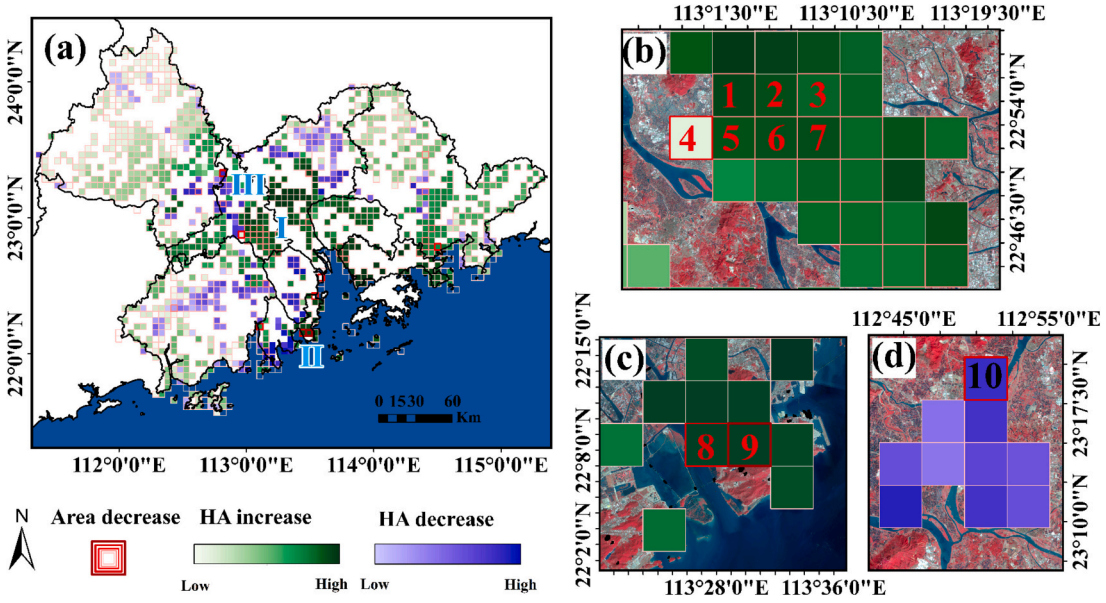

Fig. 11. (a) Coupling map of human activity changes and wetland decrease, (b) The map zoomed into location I, (c) The map zoomed into location II, (d) The map zoomed into location III.

4. Discussions

4.1. Impact of factors on the distribution and changes of wetlands

Our research indicates that FNE had a direct negative impact on WD from 1980 to 2020 because high altitude and sloping areas are not suitable for wetlands formation. Precipitation plays a role in supplementing water sources of wetlands. However, extreme precipitation may cause damage to wetlands (Xiong et al., 2023). In addition, FNE played a limiting role in HA, which in turn affected WD and WC. Fig. 4 showed that wetlands were distributed in urban areas with high HA from 1980 to 1990, while in the peripheral areas of the PRD, the WD was relatively less. The wetlands in the central area decreased significantly compared with wetlands near the outskirts of the city after 2000 (Huang et al., 2022). The results of correlation analysis and PLS–SEM reflected the same phenomenon. The direct impact of HA on WD changed from a positive impact in 1990 to a negative impact after 2000 and reached its maximum in 2010. This may be related to the intense urbanization process at that time. FNE in 1980 had a negative impact on WD through its negative impact on HA, but this impact disappeared in 1990. After 2000, FNE had a positive impact on WD through its negative impact on HA. The correlation analysis showed that Pre was negatively correlated with WD only in 1990, with a correlation coefficient of −0.39 (Fig. 7 b). However, according to PLS–SEM, Pre had a negative impact on WD in 1980, 1990, 2010, and 2020. The difference can be explained by the fact that the correlation analysis only considered values within individual grids, while PLS–SEM involved the relationships between latent and observed variables, which could reflect the causal relationships between variables. Pop/GDP were positively correlated with WD in 1980, 1990, and 2020. The reason was that the wetlands in the PRD were mainly distributed on plains, which happen to be densely populated and economically developed regions. Riv_dis was always negatively correlated with the WD from 1980 to 2020 (Fig. 7a-e, Fig. 9a-e), which was consistent with our hypothesis that the farther away from the river, the worse the water supply conditions, and the less likely wetlands were to form.

Through the violin chart (Fig. 6), it can be observed that the variables related to HA generally increased, while the WC mainly showed a decreasing trend except for 2010–2020. The HAC had a negative impact on WC from 1980 to 2010 (Fig. 10 a-c), but the impact on WC

disappeared from 2010 to 2020 because WC did not continue to decrease significantly in that period (Fig. 6-g). However, there was still some negative impact on wetlands from 2010 to 2020 (Fig. 10 d). This may be due to climate change and population growth, leading to a gradual decrease in upstream recharging and the shrinkage of surface water. The hydrological connectivity of wetlands had deteriorated, resulting in degradation. This indicated that an increase in HA led to a decrease in wetlands from 1980 to 2020 in the PRD. NNEC did not have an impact on WC from 1980 to 2010 (Fig. 10 a-c), but from 2010 to 2020 it began to pose a threat to wetlands (Fig. 10d). FNE had a positive impact on WC (mainly decrease), indicating that WC in high-altitude areas was more difficult than that in low-altitude areas. In terms of indirect impacts on WC, FNE suppressed the decrease of wetlands through negative impacts on HA. From Fig. 3, it can also be observed that the areas with reduced wetland area were located in regions with lower terrain and slopes from 1980 to 2020 because HA was relatively more intense in these areas.

4.2. Dynamic impact of human activities on non-stable natural environment

We found that the impact of HA on NNE varied in different periods, resulting in differences in its impact on WD, based on PLS–SEM (Fig. 9). Specifically, HA in 1980, 2000, and 2020 had a negative impact on WD by positively impacting NNE (Fig. 9a, c, and e). However, the negative impact of NNE had a positive impact on WD in 1990 and 2010 (Fig. 9b, d). These causal relationships may reflect correlations. For example, Pre, Tem and HA (RII, Pop, GDP, and CII) were positively correlated from 1980 to 2000, and in 2020, Tem and HA were positively correlated. The path coefficient of Pre in PLS–SEM in 2020 was 0.24, Tem was 0.998. NNE is mainly influenced by Tem. Therefore, only Tem was considered in NNE in 2020. The reason for these causal relationships may be that in the central urban areas, HA was more intense than in suburbs, and impermeable surfaces such as city roads, and buildings led to higher temperatures, which helped to form updrafts and caused frequent precipitation in these areas. The observed variables in NNE in 1990 and 2010 only included Pre and River_dis. The results showed that Pre and River_dis and HA were negatively correlated. This may be due to the peripheral effects of the urban heat island, causing moisture to fall in areas far from the city and with less HA. In addition, the effect of HAC on the decrease of wetlands through the influence of NNEC did not exist from 1980 to 2010 (Fig. 10 a-c) but exhibited negative effects during 2010–2020 (Fig. 10 d), which may exacerbate the threat to wetlands.

4.3. Advantages and disadvantages of the study

The PRD experienced rapid development after China's reform and opening up in 1978. The population has increased by about 4 times, and the GDP has increased by 76 times(Fu et al., 2023). In this study, we investigated how natural factors and HA jointly affected WD and WC in the process of rapid urbanization based on remote sensing technologies and PLS–SEM. Compared with statistical data based on administrative boundaries, remote sensing data and technologies have higher spatial resolution, can cross administrative boundaries, and provide more detailed characterization of the driving mechanisms of wetland changes. Most existing research has focused on the influencing factors of WD under static conditions; our contribution lies in the development of an asynchronous–spatiotemporal model that explains the dynamic mechanism of WC from multiple dimensions by examining the interaction between natural factors and HA (Chen et al., 2024; Fu et al., 2024; Meng et al., 2024). To our knowledge, the asynchronous–spatiotemporal model established in this study is the first attempt to examine the driving mechanisms of WC in developed urban areas since 1980. We found that there were differences in the impact of natural factors on WD and their effect on WC. Specifically, the terrain had a negative impact on WD, while changes in terrain had a positive impact on WC. This indicates that while terrain conditions limit wetlands' formation, they also protect them and prevent their destruction. NNE had a negative impact on WD but did not have an impact on WC during most periods of time. This indicates that wetlands formation is influenced by factors such as precipitation, temperature, and distance to rivers, but WC are mainly influenced by HA. The asynchronous spatiotemporal perspective proposed in this study can directly locate the impact of HAC on wetland reduction in a 5 km × 5 km grid, providing guidance for government wetland management, protection, and restoration. This study gives a detailed understanding of the WC mechanisms in the PRD over the past 40 years, giving support to government decision-making and Sustainable Development Goals.

The dominant control factors varied across different types of wetland degradation (Liu et al., 2024). Future research may consider exploring the driving factors of changes in different wetland types to guide effective and targeted coastal wetland restoration measures. Some higher-resolution earth observation data (i.e., Gaofen-1/2/4/6 WFI, Sentinel-2A/B MSI) can be used to identify different types of wetlands. Furthermore, considering that there are more factors and complex relationships that affect WD and WC, some data observations and explanations for nonlinear relationships should also be included in the model to effectively improve the simulation effect. Finally, there are differences in the impact mechanisms of HA and natural factors on wetlands in different regions. The effectiveness of the model framework in areas affected by a single condition or with more complex changes in wetland area needs to be further tested.

4.4. Comparison with other related studies in the PRD

The results of this study indicated that wetlands in the PRD experienced the largest decline in area from 1990 to 2010, while degradation approximately balanced restoration from 2010 to 2020, which is consistent with the results of Sun and Yu (2024) and Peng et al. (2024) in their study of wetland change drivers, Peng et al. adopted a sampling and visual interpretation method. Some of their findings were consistent with our conclusions, such as: 1) prior to 2010, human activities were the main cause of wetland area reduction but, from 2010 to 2020, some wetland changes were mainly influenced by the natural environment; and 2) human activities can both lead to wetland depletion and promote wetland restoration. However, Peng et al. did not analyze the influence of specific factors (e.g., population, temperature, precipitation) but rather categorized the factors into two groups (direct and indirect factors). Samples with wetland changes caused by direct factors were identified by visual interpretation, while the remaining samples were labeled as changes caused by indirect factors. Direct factors were considered to be related to human activities, while indirect factors were considered to be related to multiple natural factors. We took specific factors such as distance from the river, temperature, population, and GDP, as observed variables that affect wetlands. In addition, we explored the differences in HA intensity that promoted wetland restoration or led to wetland degradation.

Sun et al. used principal component analysis to explore the natural and anthropogenic driving forces of wetland change in the Greater Bay Area from 1980 to 2020. However, the data were from statistical yearbooks, which use administrative boundaries as statistical units and cannot reflect the heterogeneity within administrative regions. In addition, we presented for the first time the spatial distribution of the coupling relationship between human activities and wetland reduction in the PRD from 2010 to 2020. The resolution of our map was 5 km, which is particularly important for the formulation of project-based wetland restoration policies.

4.5. Implications for wetland restoration and adaptation management

The HA's intensity in this study was mainly reflected through indicators such as urban construction, economy, and population. The coupling relationship between HAC and WC revealed through PLS–SEM

from 2010 to 2020 indicated that a significant increase in HA had negative effects on wetland increase, accounting for 38.2 % of the total area. However, a small increase in HA had a positive impact on wetland increase, accounting for 39.7 %. This is because these developed areas can invest more funds in wetland restoration projects (Wu et al., 2024), and these projects directly promote the increase of wetland area, especially natural wetland area. The study by Peng et al. also indicated that the natural increase scenario, which is a baseline scenario without considering sudden policies and natural disasters, was not ideal for Greater Bay Area wetlands without policy constraints (Peng et al., 2023). Urban expansion brings economic growth, leading to investment in wetland restoration and protection funds, as well as increasing the demand for wetland landscapes due to population growth. This could result in an increase in wetlands. However, excessive urban expansion will inevitably lead to an increase in construction land and direct loss of wetland habitats.

We thus suggest that the development of wetland restoration plans should first clarify the reasons for the degradation of wetlands in the region, as well as the current threats that they face. We learned that terrain is an important factor affecting WD and WC by exploring the interactions between various driving factors over the past 40 years. Wetlands are distributed more in low-altitude areas, and WC in these areas is also greater. In addition, low-altitude areas are more strongly affected by the negative impact of HA on wetlands. Therefore, these low-altitude areas should receive more attention than high-altitude areas. Although the direct negative impact of HA on wetlands has decreased in the past decade, we should also be vigilant about the indirect negative impact of HA on wetlands through their impact on NNE in some highly developed areas.

The measures taken for wetland restoration should address the limitations of administrative boundaries and be precise to specific wetlands. We demonstrated how HA and natural factors affected the WD and WC at the scale of a 5 km × 5 km grid, revealing the spatial heterogeneity of the impact of nature and HA on wetlands. The process of HA and its impact on wetlands destruction and restoration is delayed. The coupling relationship between HA and WC reflected from 2010 to 2020 can also provide references for the current government's refined formulation of wetland restoration plans. Therefore, we propose specific adaptations for the current situation. For example, the increase in HA in the southeast of Foshan has led to a more serious phenomenon of wetland decrease than other areas in the PRD. Therefore, more attention, such as establishing wetland reserves and limiting the maximum capacity of wetland parks, should be paid to conserving wetlands during urbanization to reduce the impact of HA on wetland loss. At the junction of Zhaoqing and Foshan, HA decreased but the wetland also decreased. Therefore, these areas should focus on the importance of natural environmental factors in WC and can develop their economy appropriately to invest in improving the natural environment.

In 2019, the United Nations proposed the period 2021–2030 as the Decade of Ecosystem Restoration. In 2022, the Kunming Montreal Global Biodiversity Framework set a goal of restoring over 30 % of degraded ecosystems by 2030. In the context of global wetland restoration, regions with rapid economic and urbanization development should pay attention to the negative impact of HA on wetlands. For regions that prioritize development quality, successful wetland restoration is related to social and public participation, and the best restoration approach should combine active restoration (vegetation management, topography modification, hydraulic regulation) with passive restoration. In addition, it is necessary to choose appropriate restoration methods based on factors such as restoration goals, wetland degradation degree, causes, and funding in the actual restoration process.

5. Conclusions

This study explored the driving mechanisms between factors (HA, NNE, and FNE) and wetlands (WD and WC). The model integrated remote sensing technologies and PLS–SEM. We applied the model to the PRD, achieving good explanatory accuracy. The CR of the model was greater than 0.6, and the AVE was greater than 0.5. Then, we explored the coupling relationship between HA and WC and proposed suggestions for wetland restoration management. The remote sensing classification results showed that the wetland area in the PRD decreased by 50 % from 1980 to 2020, with the largest decrease of 41 % from 1990 to 2000, and relative stability after 2010. The pathways that affect wetlands indicated that HA had had a negative impact on WD and WC from 1980 to 2010, and both negative and positive impacts since 2010. NNE has negatively affected WD since 2010. FNE can limit HAC and inhibit its negative impact on wetlands, protecting them from damage. HA can affect NNE and subsequently affect WD, but only after 2010 did this begin to have an impact on the decrease of wetlands. We suggest that HA should be restricted in the coastal areas of southeastern Foshan and northeastern Zhuhai to protect wetlands. We expect the proposed model to be applied in other areas where wetlands are significantly under threat from the natural environment and HA. In the future, the differences in driving mechanisms of different wetland types should be considered to better explain WD and WC.

CRediT authorship contribution statement

Xiaoqing Yi: Writing – review & editing, Project administration, Methodology, Investigation, Conceptualization. **Yuhang Wang:** Writing – review & editing, Writing – original draft, Methodology, Investigation, Formal analysis, Data curation, Conceptualization. **Changjun Gao:** Writing – review & editing, Project administration, Methodology, Investigation, Conceptualization. **Jiaojiao Ma:** Project administration, Investigation. **Demin Zhou:** Project administration, Investigation. **Christian J. Sanders:** Writing – review & editing, Project administration. **Guangjia Jiang:** Project administration. **Zhongwen Hu:** Project administration. **Junjie Wang:** Project administration. **Haichao Zhou:** Resources. **Wei Li:** Resources.

Data availability

Data will be made available on request.

Acknowledgments

We acknowledge the Guangdong forestry science and technology innovation project (No. 2021KJCX0051), the Guangdong Basic and Applied Basic Research Foundation (No. 2021A1515011670), and the National Natural Science Foundation of China (No. 42201076). We thank Leonie Seabrook, PhD, from Liwen Bianji (Edanz) (www.liwenbianji.cn), for editing the English text of a draft of this manuscript.

Appendix A. Supplementary data

Supplementary data to this article can be found online at https://doi.org/10.1016/j.ecoinf.2024.102979.

References

Aktas, N.K., Donmez, N.Y., 2019. Effects of urbanisation and human activities on basin ecosystem: Sapanca Lake Basin. J. Environ. Prot. Ecol. 20 (1), 102–112.

Asselen, S.V., Verburg, P.H., Vermaat, J.E., Janse, J.H., 2013. Drivers of wetland conversion: a global meta-analysis: e81292. PLoS One 8 (11). https://doi.org/10.1371/journal.pone.0081292.

Bunting, P., Rosenqvist, A., Hilarides, L., Lucas, R.M., Thomas, N., Tadono, T., et al., 2022. Global mangrove extent change 1996–2020: global mangrove watch version 3.0. Remote Sens. 14 (15), 3657. https://doi.org/10.3390/rs14153657.

Chen, L., Jin, Z., Michishita, R., Cai, J., Yue, T., Chen, B., et al., 2014. Dynamic monitoring of wetland cover changes using time-series remote sensing imagery. Ecol. Inform. 24, 17–26. https://doi.org/10.1016/j.ecoinf.2014.06.007.

Chen, K., Dong, Z., Gong, J., 2024. Monitoring dynamic mangrove landscape patterns in China: effects of natural and anthropogenic forcings during 1985–2020. Ecol. Inform. 81, 102582. https://doi.org/10.1016/j.ecoinf.2024.102582.

Cui, L., Gao, C., Zhou, D., Mu, L., 2014. Quantitative analysis of the driving forces causing declines in marsh wetland landscapes in the Honghe region, Northeast China, from 1975 to 2006. Environ. Earth Sci. 71 (3), 1357–1367. https://doi.org/10.1007/s12665-013-2542-5.

Deng, Y., Shao, Z., Dang, C., Huang, X., Wu, W., Zhuang, Q., et al., 2023. Assessing urban wetlands dynamics in Wuhan and Nanchang, China. Sci. Total Environ. 901, 165777. https://doi.org/10.1016/j.scitotenv.2023.165777.

Erwin, K.L., 2009. Wetlands and global climate change: the role of wetland restoration in a changing world. Wetl. Ecol. Manag. 17 (1), 71–84. https://doi.org/10.1007/s11273-008-9119-1.

Fluet-Chouinard, E., Stocker, B.D., Zhang, Z., Malhotra, A., Melton, J.R., Poulter, B., et al., 2023. Extensive global wetland loss over the past three centuries. Nature 614 (7947), 281–286. https://doi.org/10.1038/s41586-022-05572-6.

Fu, Y., Lin, Q., Grifoll, M., Lam, J.S.L., Feng, H., 2023. Investigating the evolution of the Guangdong-Hong Kong-Macao Greater Bay Area (GBA) multi-port system: the multi-faced perspectives. Ocean Coast. Manag. 233, 106450. https://doi.org/10.1016/j.ocecoaman.2022.106450.

Fu, M., Zheng, Y., Qian, C., He, Q., He, Y., Wei, C., et al., 2024. Spatiotemporal evolution and driving mechanism of Dongting Lake based on 2005–2020 multi-source remote sensing data. Ecol. Inform. 83, 102822. https://doi.org/10.1016/j.ecoinf.2024.102822.

Hair, J.F., Ringle, C.M., Sarstedt, M., 2011. PLS-SEM: indeed a silver bullet. J. Market. Theory Pract. 2 (19), 139–152.

Hayes, A.F., Montoya, A.K., Rockwood, N.J., 2017. The analysis of mechanisms and their contingencies: PROCESS versus structural equation Modeling. Australas. Mark. J. 25 (1), 76–81. https://doi.org/10.1016/j.ausmj.2017.02.001.

Hu, S., Niu, Z., Chen, Y., Li, L., Zhang, H., 2017. Global wetlands: potential distribution, wetland loss, and status. Sci. Total Environ. 586, 319–327. https://doi.org/10.1016/j.scitotenv.2017.02.001.

Huang, X., Wu, Z., Zhang, Q., Cao, Z., 2022. How to measure wetland destruction and risk: wetland damage index. Ecol. Indic. 141, 109126. https://doi.org/10.1016/j.ecolind.2022.109126.

Jia, M., Wang, Z., Mao, D., Ren, C., Song, K., Zhao, C., et al., 2023. Mapping global distribution of mangrove forests at 10-m resolution. Sci. Bull. 68 (12), 1306–1316. https://doi.org/10.1016/j.scib.2023.05.004.

Li, S., Wu, J., Gong, J., Li, S., 2018. Human footprint in Tibet: assessing the spatial layout and effectiveness of nature reserves. Sci. Total Environ. 621, 18–29. https://doi.org/10.1016/j.scitotenv.2017.11.216.

Li, Z., Liu, M., Hu, Y., Xue, Z., Sui, J., 2020. The spatiotemporal changes of marshland and the driving forces in the Sanjiang plain, Northeast China from 1980 to 2016. Ecol. Process. 9 (1). https://doi.org/10.1186/s13717-020-00226-9.

Li, H., Wang, J., Zhang, J., Qin, F., Hu, J., Zhou, Z., 2021. Analysis of characteristics and driving factors of wetland landscape pattern change in Henan Province from 1980 to 2015. Land 10 (6), 564. https://doi.org/10.3390/land10060564.

Li, Y., Hou, Z., Zhang, L., Qu, Y., Zhou, G., Lin, J., et al., 2023. Long-term spatio-temporal changes of wetlands in Tibetan plateau and their response to climate change. Int. J. Appl. Earth Obs. Geoinf. 121, 103351. https://doi.org/10.1016/j.jag.2023.103351.

Liu, H., Jiang, D., Luo, X., Yang, C., 2005. Spatialization approach to 1km grid GDP supported by remote sensing. Geo-Inform. Sci. 7 (2), 120–123.

Liu, C., Yuan, X., Ni, G., Liu, Y., Qi, Y., Miao, S., 2024. Utilizing deep transfer learning to discover changes in landscape patterns in urban wetland parks based on multispectral remote sensing. Ecol. Inform. 83, 102808. https://doi.org/10.1016/j.ecoinf.2024.102808.

Lu, W., Xu, C., Wu, J., Cheng, S., 2019. Ecological effect assessment based on the DPSIR model of a polluted urban river during restoration: a case study of the Nanfei River, China. Ecol. Indic. 96, 146–152. https://doi.org/10.1016/j.ecolind.2018.08.054.

Ma, J., Loiselle, S., Cao, Z., Qi, T., Shen, M., Luo, J., et al., 2023. Unbalanced impacts of nature and nurture factors on the phenology, area and intensity of algal blooms in global large lakes: MODIS observations. Sci. Total Environ. 880, 163376. https://doi.org/10.1016/j.scitotenv.2023.163376.

Mao, Y., Xin, C., Rong, J., 2021. The agglomeration and diffusion mechanism and spatial structure characteristics of central cities in the Guangdong-Hong Kong-Macao Greater Bay area. J. South China Norm. Univ. (Soc. Sci. Ed.) 66 (6), 26–37.

Mcowen, C., Weatherdon, L., Bochove, J., Sullivan, E., Blyth, S., Zockler, C., et al., 2017. A global map of saltmarshes. Biodivers. Data J. 5, e11764. https://doi.org/10.3897/BDJ.5.e11764.

Meng, H., Zhang, J., Zheng, Z., Song, Y., Lai, Y., 2024. Classification of inland lake water quality levels based on Sentinel-2 images using convolutional neural networks and spatiotemporal variation and driving factors of algal bloom. Ecol. Inform. 80, 102549. https://doi.org/10.1016/j.ecoinf.2024.102549.

Murray, N.J., Worthington, T.A., Bunting, P., Duce, S., Hagger, V., Lovelock, C.E., et al., 2022. Science-high-resolution mapping of losses and gains of Earth's tidal wetlands. Science 6594 (376), 744–749. https://doi.org/10.1126/science.abm9583.

Omann, I., Stocker, A., Jäger, J., 2009. Climate change as a threat to biodiversity: an application of the DPSIR approach. Ecol. Econ. 69 (1), 24–31. https://doi.org/10.1016/j.ecolecon.2009.01.003.

Peng, K., Jiang, W., Wang, X., Hou, P., Wu, Z., Cui, T., 2023. Evaluation of future wetland changes under optimal scenarios and land degradation neutrality analysis in the Guangdong-Hong Kong-Macao Greater Bay Area. Sci. Total Environ. 879, 163111. https://doi.org/10.1016/j.scitotenv.2023.163111.

Peng, K., Jiang, W., Hou, P., Cui, T., Wu, Z., Si, B., 2024. Exploring the long-term dynamics of detailed wetland types and their driving forces in coastal metropolitan areas from 1990 to 2020. Int. J. Appl. Earth Obs. Geoinf. 132, 104012. https://doi.org/10.1016/j.jag.2024.104012.

Pickens, A.H., Hansen, M.C., Hancher, M., Stehman, S.V., Tyukavina, A., Potapov, P., et al., 2020. Mapping and sampling to characterize global inland water dynamics from 1999 to 2018 with full Landsat time-series. Remote Sens. Environ. 243, 111792. https://doi.org/10.1016/j.rse.2020.111792.

Sterling, S.M., Ducharne, A., Polcher, J., 2013. The impact of global land-cover change on the terrestrial water cycle. Nat. Clim. Chang. 3 (4), 385–390. https://doi.org/10.1038/nclimate1690.

Sun, K., Yu, W., 2024. A satellite view of the wetland transformation path and associated drivers in the Greater Bay Area of China during the past four decades. Remote Sens. 16 (6), 1047. https://doi.org/10.3390/rs16061047.

Tan, L., Ge, Z., Li, S., Zhou, K., Lai, D.Y.F., Temmerman, S., et al., 2023. Impacts of land-use change on carbon dynamics in China's coastal wetlands. Sci. Total Environ. 890, 164206. https://doi.org/10.1016/j.scitotenv.2023.164206.

Thomas, N., Lucas, R., Bunting, P., Hardy, A., Rosenqvist, A., Simard, M., 2017. Distribution and drivers of global mangrove forest change, 1996–2010. PLoS One 12 (6), e0179302. https://doi.org/10.1371/journal.pone.0179302.

Wang, X., Wu, J., Wang, H., Li, N., 2016. Comparison of GDP Spatialization in Beijing-Tianjin-Hebei based on night light and population density data. J. Geo-Inform. Sci. 18 (7), 969–976. https://doi.org/10.3724/SP.J.1047.2016.00969.

Wang, C., Ma, L., Zhang, Y., Chen, N., Wang, W., 2022a. Spatiotemporal dynamics of wetlands and their driving factors based on PLS-SEM: a case study in Wuhan. Sci. Total Environ. 806, 151310. https://doi.org/10.1016/j.scitotenv.2021.151310.

Wang, J., Teng, D., He, X., Li, Z., Chen, Y., Ma, W., et al., 2022b. Spatial variation in the direct and indirect effects of plant diversity on soil respiration in an arid region. Ecol. Indic. 142, 109288. https://doi.org/10.1016/j.ecolind.2022.109288.

Wang, Y., Wang, X., Khan, S., Zhou, D., Ke, Y., 2023. Evaluation of mangrove restoration effectiveness using remote sensing indices - a case study in Guangxi Shankou mangrove National Natural Reserve, China. Front. Mar. Sci. 10. https://doi.org/10.3389/fmars.2023.1280373.

Winkler, M.G., Dewitt, C.B., 1985. Environmental impacts of peat Mining in the United States: documentation for wetland conservation. Environ. Conserv. 12 (4), 317–330. https://doi.org/10.1017/S0376892900034433.

Wu, Y., Wang, J., Gou, A., 2024. Research on the evolution characteristics, driving mechanisms and multi-scenario simulation of habitat quality in the Guangdong-Hong Kong-Macao Greater Bay based on multi-model coupling. Sci. Total Environ. 924, 171263. https://doi.org/10.1016/j.scitotenv.2024.171263.

Xiong, Y., Mo, S., Wu, H., Qu, X., Liu, Y., Zhou, L., 2023. Influence of human activities and climate change on wetland landscape pattern—a review. Sci. Total Environ. 879, 163112. https://doi.org/10.1016/j.scitotenv.2023.163112.

Xu, D., Bisht, G., Tan, Z., Sinha, E., Di Vittorio, A.V., Zhou, T., et al., 2024. Climate change will reduce north American inland wetland areas and disrupt their seasonal regimes. Nat. Commun. 15 (1). https://doi.org/10.1038/s41467-024-45286-z.

Yang, L., Shen, F., Zhang, L., Cai, Y., Yi, F., Zhou, C., 2021. Quantifying influences of natural and anthropogenic factors on vegetation changes using structural equation modeling: a case study in Jiangsu Province, China. J. Clean. Prod. 280, 124330. https://doi.org/10.1016/j.jclepro.2020.124330.

Zedler, J.B., Kercher, S., 2005. Wetland resources: status, trends, ecosystem services, and restorability. Annu. Rev. Environ. Resour. 30 (1), 39–74. https://doi.org/10.1146/annurev.energy.30.050504.144248.

Zhang, X., 2015. Climate change impacts on wetlands of the Yellow River headwaters. Nat. Environ. Pollut. Technol. 14 (2), 217–226.

Zhang, M., Lin, H., Long, X., Cai, Y., 2021. Analyzing the spatiotemporal pattern and driving factors of wetland vegetation changes using 2000-2019 time-series Landsat data. Sci. Total Environ. 780, 146615. https://doi.org/10.1016/j.scitotenv.2021.146615.

Zhang, J., Qin, Y., Zhang, Y., Lu, X., Cao, J., 2023a. Comparative assessment of the spatiotemporal dynamics and driving forces of natural and constructed wetlands in arid and semiarid areas of northern China. Land 12 (11), 1980. https://doi.org/10.3390/land12111980.

Zhang, Z., Jiang, W., Peng, K., Wu, Z., Ling, Z., Li, Z., 2023b. Assessment of the impact of wetland changes on carbon storage in coastal urban agglomerations from 1990 to 2035 in support of SDG15.1. Sci. Total Environ. 877, 162824. https://doi.org/10.1016/j.scitotenv.2023.162824.

Zhang, X., Liu, L., Zhao, T., Wang, J., Liu, W., Chen, X., 2024. Global annual wetland dataset at 30 m with a fine classification system from 2000 to 2022. Sci. Data 11 (1). https://doi.org/10.1038/s41597-024-03143-0.